Journal of Molecular Structure 1122 (2016) 198–204

Contents lists available at ScienceDirect

Journal of Molecular Structure

journal homepage: http://www.elsevier.com/locate/molstruc

Raman and surface enhanced Raman scattering study of the orientation of cruciform 9,10-anthracene thiophene and furan derivatives deposited on a gold colloidal surface

J. Muñoz-Pérez [a], P. Leyton [a, *], C. Paipa [a], J.P. Soto [a], J. Brunet [a], J.S. Gómez-Jeria [b], M.M. Campos-Vallette [b]

[a] Instituto de Química, Pontificia Universidad Católica de Valparaíso, Valparaíso, Chile
[b] Laboratorio de Espectroscopía Vibracional, Departamento de Química, Facultad de Ciencias, Universidad de Chile, P.O. Box 653, Santiago, Chile

ARTICLE INFO

Article history:
Received 10 February 2016
Received in revised form
4 May 2016
Accepted 1 June 2016
Available online 2 June 2016

Keywords:
Raman spectrum
Surface-enhanced Raman scattering
Cruciform
Gold cluster

ABSTRACT

The 9,10-di(thiophen-2-yl)anthracene (TAT), 9,10-di(furan-2-yl)anthracene (FAF) and 2-[(10-(thiophen-2-yl)anthracen-9-yl)]furan (TAF) cruciform molecular systems were synthesized using one-step coupling reactions and structurally characterized via Raman, infrared, ^{1}H NMR, ^{13}C NMR and mass spectroscopies. The orientation of the analytes on a gold colloidal surface was inferred from a surface-enhanced Raman scattering (SERS) study. The metal surface interaction was driven by the S and O atoms of the thiophene and furan α-substituents, and the plane of the anthracene fragment remained parallel to the surface. Theoretical calculations based on a simplified molecular model for the analyte-surface interaction provide a good representation of the experimental data.

1. Introduction

Recently, metallic or semiconductor nanoparticle fabrication and modification techniques have been developed to produce surfaces with suitable properties for use in electronic, optical and spectroscopic devices [1–3]. The design of these devices often requires the immobilization of a molecular system on the surface of a nanostructure or continuous metallic surfaces via specific chemical adsorption [4,5] or self-aggregation mechanisms [6]. Therefore, the rational design of this type of molecular device has been focused on molecular electronics applications, such as molecular wires, rectifiers, switches, transistors and sensors that have the ability to selectively recognize a certain type of substrate. Self-assembled monolayers consisting of conjugated organic molecules have generated much interest due to their electronic conduction controlled by the functional groups at the ends of the structure [7].

In comparison to the extensively developed chemistry of self-assembled monolayers (SAM) of aliphatic organic molecules on a surface, relatively few studies on homologous aromatic building blocks have been performed. Studies on bi-dimensional aromatic conjugated compounds of a considerable size adsorbed on metallic surfaces are also scarce. A significant issue for applications involving simple aromatic molecules, especially for aromatic thiols and dithiols, involves the assumption that the formed films have a specific orientation on the surface. The orientation is dependent on thermodynamic and kinetic factors, which directly influence the vertical growth of the monolayer and limit the potential applications of these systems [8–12].

Currently, surface-enhanced Raman spectroscopy (SERS) has become a powerful technique for use in various areas (e.g., biology, cultural heritage, and environmental pollution). The characteristics of this technique include its high sensitivity. This behavior is primarily due to the substantial electromagnetic enhancement from the nanostructured metal surfaces, and the resonance effect associated with adsorbate-metal charge transfer.

However, one of the most attractive results obtained from the technique involves the ability to gain insight into the orientation of molecules that are adsorbed onto metallic nanostructured surfaces. Intensity changes due to surface effects are interpreted based on the SERS selection rules [13,14]; modes with a Raman polarizability z-component that is perpendicular to the surface are most likely to be more enhanced than the parallel ones. Therefore, the orientation and organization of the analytes on the metal surface can be

* Corresponding author.
E-mail address: patricio.leyton@pucv.cl (P. Leyton).

http://dx.doi.org/10.1016/j.molstruc.2016.06.002
0022-2860/

inferred. The spectral shifting observed due to surface effects for some bands is related to a probable electronic charge transfer resulting from the ligand-metal surface interaction.

It is important to note that polycyclic aromatic hydrocarbons, such as anthracene, do not exhibit a SERS spectrum except when molecular assemblers are used [15,16]. Both furan and thiophene compounds exhibit SERS effect when deposited on various nanostructured metal surfaces [17–19]. Therefore, the furan and thiophene substituents in positions 9 and 10 in anthracene may drive or allow the approximation of the whole molecular system relative to the metal surface. In addition, SERS possesses unique features that make it a suitable tool for the study the basic aspects of molecular devices involving metal contacts, such as substrate-adsorbate interactions and molecular orientations on nanostructured metal surfaces.

Here, we performed a systematic study of the molecular structure, orientation and organization on gold colloidal nanoparticles of a family of cruciform molecular derivatives of 9,10-dibromoanthracene: 9,10-di(thiophen-2-yl)anthracene (TAT), 9,10-di(furan-2-yl)anthracene (FAF) and 2-[(10-(thiophen-2-yl) anthracen-9-yl)]furan (TAF) (Fig. 1). The main goal was to clarify the molecular origin of the self-aggregation process in order to control the supramolecular organization of organic molecules. Gaining an understanding of these factors is a pre-requisite for the development of new methodologies to fabricate molecular aggregates on surfaces with a definite structure. The present contribution could give insights on the fabrication of molecular electronics devices or specific sensors.

2. Experimental section

2.1. Synthesis of gold nanoparticles

All of the solutions were prepared using water obtained from a Milli-Q Simplicity system (Millipore), which produced water with a resistivity in the 10–15 MΩ × cm range. Gold nanoparticles (Au-NP) were obtained by citrate reduction of $HAuCl_4$ using the Frens method [20].

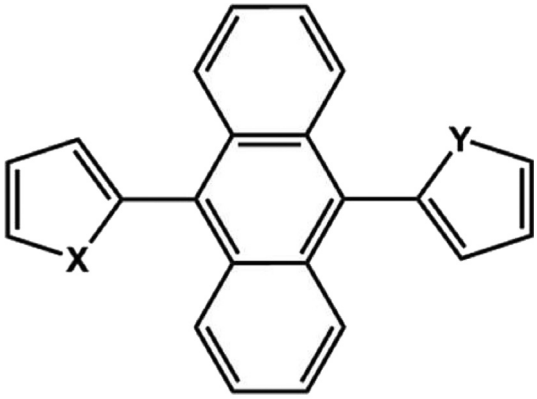

	X	Y
TAT	S	S
FAF	O	O
TAF	S	O

Fig. 1. Family of cruciform molecular derivatives from 9,10-dibromoanthracene: 9,10-di(thiophen-2-yl)anthracene (TAT), 9,10-di(furan-2-yl)anthracene (FAF) and 2-[(10-(thiophen-2-yl)anthracen-9-yl)]furan (TAF).

2.2. Synthesis of symmetrical and unsymmetrical 9,10-diarylanthracene derivatives

9,10-Di(thiophen-2-yl)anthracene (TAT), 9,10-di(furan-2-yl) anthracene (FAF) and 2-[(10-(thiophen-2-yl)anthracen-9-yl)]furan (TAF) were synthesized using a previously published protocol by Durso et al. [21] and Kotha et al. [22] with modifications via Grignard reagent (supplementary material S1). The characterization of the obtained products is in agreement with that reported by the authors.

2.3. Instrumentation

The IR spectra were recorded on a JASCO FTIR-4600 spectrometer equipped with a DLA-TGS detector (deuterated L-alanine doped triglycine sulfate) with Peltier temperature control. The spectral resolution was 4 cm^{-1} and 32 scans were performed. IR spectral data along with the assignment of the most intense bands are available as supplementary material S1.

The Raman and SERS spectra were obtained using a Witec Alpha 300 confocal Raman microscope system equipped using an excitation laser wavelength of 785 nm and an electrically cooled CCD camera. The signal was calibrated using the 520 cm^{-1} line of a Si wafer and a 20× objective. The laser power on the samples was 2 mW. The resolution was set to 4 cm^{-1} and 20 scans with an integration time of 1 s were performed. The spectra were recorded over the 200–1800 cm^{-1} region. All of the samples were photostable when probed at 785 nm.

2.4. Computational details

Similar to our previous studies, we simulated the gold surface by constructing a large Au cluster with a face centered-cubic structure using the Hyperchem software [23]. Briefly, a large face centered-cubic structure with a = 0.4786 nm was built and trimmed to get a planar double layer composed of 512 gold atoms. The geometry optimization was carried out at the OPLS level by keeping constant the bilayer geometry and by letting evolve the probe molecules over the rigid Au surface. TAT (TAF) were placed at different distances and orientations from the center of the Au bilayer. No solvent was included in the optimization procedure because the direct molecule-surface interaction was modeled, which is required to obtain the SERS spectrum (the other condition involves the molecule-metal interaction occurring on a hot spot). Extended Hückel theory (EHT) was employed to calculate the wave function of the molecules as isolated systems as well as interacting with the metal surface. EHT was chosen because within the Hartree–Fock–Rüdenberg representation, EHT is compatible with the nonempirical Hartree–Fock method in Roothaan's form.

On the other hand, the electronic structure of the molecules was calculated at the B3LYP/6-31G(d,p) level with the Gaussian suite of programs with full geometry optimization [24]. This last calculation provided the HOMO and LUMO structures and energies together with the IR and Raman spectra. This approach provided qualitative explanations of our previous SERS results for several different molecular systems interacting with Ag or Au surfaces [25–31]. Further information is available as Supplementary material S2.

3. Results and discussion

3.1. Raman spectral analysis

3.1.1. Bands assignment

The Raman band assignment for TAT, FAF and TAF was performed using general spectral information [32–34] and analysis of

the vibrational spectra of anthracene [35] and naphthalene based on density functional calculations by Lokshin et al. [36] and Srivastava and Singh [37] as well as vibrational analysis of furan and thiophene spectra reported by El-Azhary et al. [38]. The analysis was performed for the 1800–200 cm^{-1} spectral region (Fig. 2). Table 1 displays the most probable Raman bands assignment of the cruciform molecular systems. The bands at 1588 and 1498 cm^{-1} were only observed in the spectra for FAF and TAF, in the last case the unsymmetrical derivative indicates a frequency shift to 1597 and 1505 cm^{-1}, respectively due to the furan moiety, especially the aromatic νCC mode. The weak band located at 1372 cm^{-1}, is assigned to a coupled νCC ring/CH deformation (δCH) mode of the furane moiety. The strong band at approximately 1563 cm^{-1} was most likely due a vibration containing an important contribution from νCC modes from the thiophene and furan substituents. This band was observed at 1563 cm^{-1} for TAT, 1557 cm^{-1} for FAF and 1559 cm^{-1} for TAF. The band located at 1539 cm^{-1} for TAT, which was observed at similar wavenumbers for FAF and TAF, was due to νCC modes of the anthracene ring. The shoulder at 1529 cm^{-1} was only observed for TAT, which suggests a thiophene vibration νCC mode. In the three molecular systems, the weak band that was observed at approximately 1484 cm^{-1} was a coupled mode consisting of δCH and νCC modes from the anthracene moiety. The weak medium bands at 1439 and 1350 cm^{-1} of TAT and 1443 and 1350 cm^{-1} of TAF correspond to thiophene vibrations involving the δCH and νCC modes, the medium band at 1079 cm^{-1} in TAT and 1074 cm^{-1} in TAF, are mainly δCH modes of thiophene. The strong bands located at 1410 and 1286 cm^{-1} for FAF are observed in TAT at 1406 and 1279 cm^{-1}, respectively. This spectral behavior is associated with the mass effect of the furan and thiophene substituents. Therefore, the corresponding vibration should contain information regarding modes involving the corresponding O and S heteroatoms. The weak bands located at 1217 and 1176 cm^{-1} and the medium band at 1022 cm^{-1} which were observed in all three systems, were due to coupled δCH/νCC modes of the anthracene component. A similar assignment is proposed for the weak bands in the 1000–900 cm^{-1} range. Several weak medium bands were observed in the 900–780 cm^{-1} range, and the spectral behavior suggests that these bands may be due to ring deformations and out-of-plane CH deformations (ρCH) of the anthracene, thiophene and furan rings. In fact, the band located at 867 cm^{-1} was observed for TAT and TAF and corresponded to thiophene vibrations. However, the band located at 820 cm^{-1} was observed for TAT and at 836 cm^{-1} for FAF and corresponded to an anthracene vibration. The medium bands at 746 cm^{-1} in TAT, and at 744 cm^{-1} in TAF correspond to a thiophene ρCH. The observed wavenumber shifting of the thiophene and furan bands in the 710–670 cm^{-1} range was associated to vibrational modes involving the COC and CSC molecular fragments. The bands located at approximately 670 and 600 cm^{-1} in the TAT,

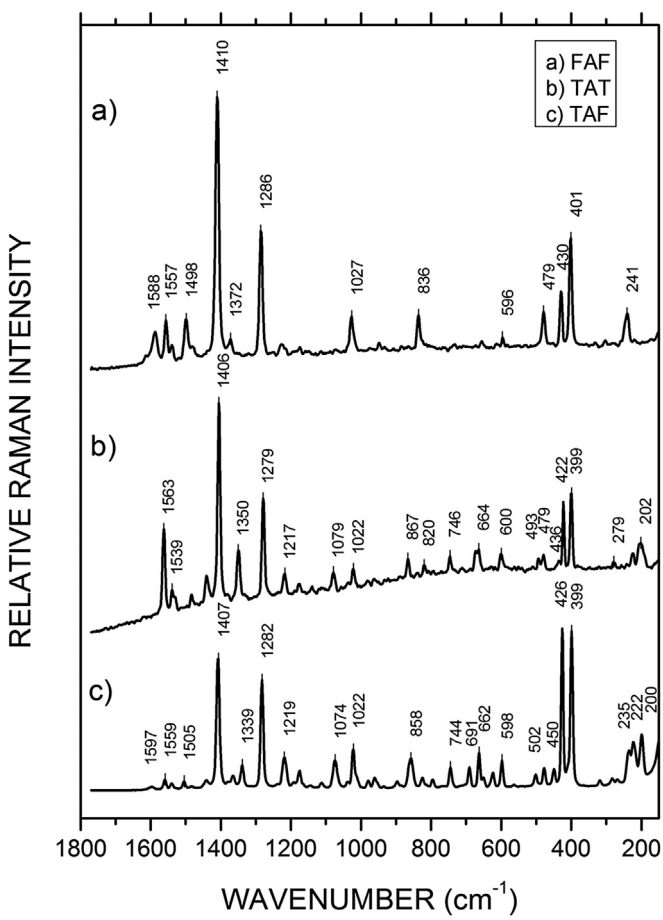

Fig. 2. Raman spectra of the solids of the cruciform systems: a) FAF, b) TAT and c) TAF.

Table 1
Raman and SERS wavenumbers (cm^{-1}) and the most probable bands assignment of the cruciform systems in the 1800–200 cm^{-1} spectral region.

Raman[a]			SERS			Bands assignment[b]
TAT	FAF	TAF	TAT	FAF	TAF	
	1588m	1597vw		1601m	1588w	νCC_F
1563s	1557m	1559vw	1563m	1560m	1560m	νCC_F, νCC_T
1539m	1540w	1540vw	1539w	1542w	1538w	νCC_A
1529sh						νCC_T
n.d.	1498m	1505vw		1504w	1504vw	νCC_F
1484w	1480w	1483vw				$\nu CC/\delta CH_A$
1439m		1443vw	1439m			$\nu CC/\delta CH_T$
1406vs	1410vs	1407vs	1406s	1410s	1391s	νCC_F, νCC_T
	1372w			1370w		$\nu CC/\delta CH_F$
1350m		1339m	1350w			$\nu CC/\delta CH_T$
1279s	1286s	1282s	1279m	1286s	1294m	νCC_F, νCC_T
					1271w	νCC_F, νCC_T
1217m	1222w	1219m				$\delta CH/\nu CC_A$
					1183m	$\delta CH/\nu CC_F$, νCC_T
1176vw	1176vw	1176vw				$\delta CH/\nu CC_A$
					1161m	$\delta CH/\nu CC_F$, νCC_T
1079m		1074m				δCH_T
1022m	1027m	1022m				$\delta CH/\nu CC_A$
979w	976w	979w				$\delta CH/\nu CC_A$
958vw	950vw	961w				$\delta CH/\nu CC_A$
887vw	884vw	896w				ring def.
867m		858m				ρCH_T
820w	836m	824w				ρCH_A
746m		744m				ρCH_T
689vw		691w				ring def.$_T$, ring def.$_F$
672sh		669sh	670m			ring def.$_T$, ring def.$_F$
664m		662m				$\rho CH_{T,F}$
600m	596vw	598m				$\rho CH_{T,F}$
493w		502w		498w	489w	ring def.$_T$, ring def.$_F$
479w	479m	477w		463w	475w	ring def.$_A$
		450w		446w		ring def.$_T$, ring def.$_F$
436vw			438m			ρCH_T
422s	430m	426s	422m	428m	424m	ring def.$_T$, ring def.$_F$
399s	401s	399s	401m	401m	403w	ring def. $_A$
					369 w	νAuO
					276w	νAuS
	241m	235sh		239m	239w	ring def.$_F$
226w		222m				ring def.$_T$,
202m		200m	202w			ring def.$_T$

[a] Symbols refer to signal intensity, and the legend of symbols is as follows: vs, very strong; s, strong; m, medium; w, weak; vw, very weak; sh, shoulder.
[b] Symbols refer to vibrational modes, and legend of symbols is as follows: ν, stretching; δ, in plane deformation; ρ, out of plane deformation; A, anthracene ring; F, furan ring; T, thiophene ring.

TAF and FAF spectra could be associated to ρCH deformations. The bands at 502 and 450 cm^{-1} in TAF and 493 and 436 cm^{-1} in TAT corresponded to the same vibration (i.e., a ring deformation), involving O and S atoms, respectively. The mass effect caused the observed wavenumber shift. The bands at 479 and 399 cm^{-1} maintain the same wavenumber in all three cases; these bands correspond to the anthracene fragment and most likely out-of-plane ring deformations. In contrast, the strong band located at approximately 430 cm^{-1} shifts to a lower wavenumber due to the mass effect, which indicates that the corresponding vibrational mode corresponds to a structural fragment of heterocycles involving the O and S atoms. The bands at 241 cm^{-1} for FAF and 226 cm^{-1} for TAT were due to ring deformations involving heteroatoms. In TAF, the first band was observed at 235 cm^{-1}, and the thiophene band was observed at 222 cm^{-1}. The broad band located at 202 cm^{-1} for TAT and 200 cm^{-1} for TAF may be primarily due to a thiophene vibration, and no bands were observed for FAF.

3.2. SERS spectral analysis

The SERS spectral profiles of the TAT, FAF and TAF molecules are similar (Fig. 3). The similarities are primarily related to bands corresponding to the anthracene moiety, and the differences are related to vibrations of the heterocyclic substituents. In fact, the furan bands at 1588 and 1498 cm^{-1} remain in the SERS spectrum with a slight shift to 1601 and 1504 cm^{-1}, respectively; see Table 1. The relative intensity of the first band increased due to the surface effect, and the intensity of the second band decreased. According the SERS selection rules [13,14], these bands should correspond to νCC modes vibrating tilted or perpendicular to the metal surface.

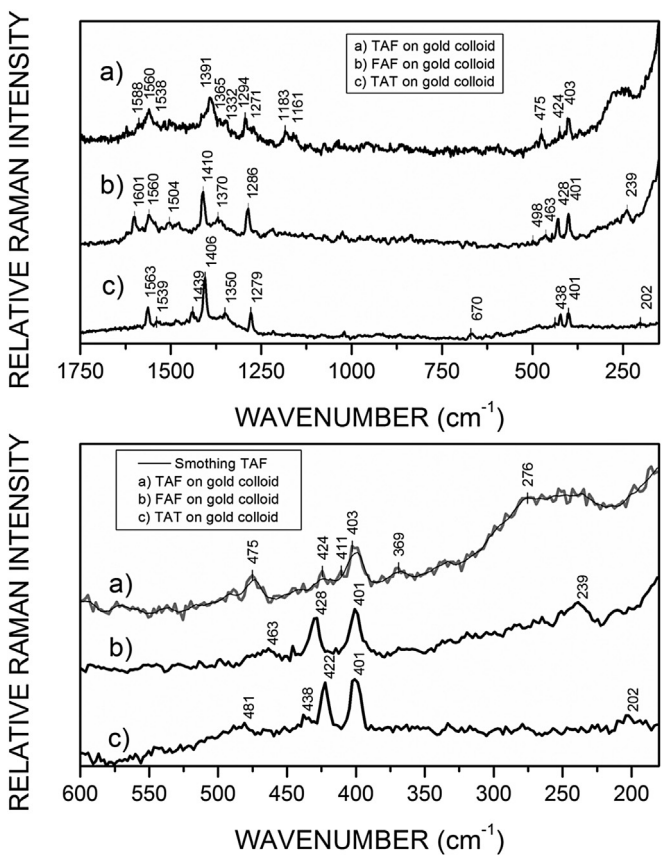

Fig. 3. SERS spectra of a) TAF, b) FAF and c) TAT, on gold nanoparticles, in the 1800–200 cm^{-1} region (top) and 600–200 cm^{-1} region (bottom).

The wavenumber shift was associated with a probable charge transfer of the entire molecular system interacting with the metal surface. The anthracene weak band at 1539 cm^{-1} remained at a similar wavenumber with a very low intensity due to surface effects in the three molecules. Therefore, the aromatic molecular fragment of anthracene is most likely far from the surface and inclined relative to the surface. The coupled νCC/δCH mode of thiophene at 1439 and 1350 cm^{-1} was observed with a low intensity in the SERS spectrum of TAT and maintaining the same wavenumber. This mode was not observed for TAF. Based on this spectral behavior, the thiophene ring is most likely perpendicular to the surface in TAT but less perpendicular in TAF. The strong bands for FAF at 1410 and 1286 cm^{-1} and in TAT at 1406 and 1279 cm^{-1} maintained their intensities and wavenumber due to the surface effect. If these bands correspond to νCC modes, and the anthracene moiety is parallel to the surface, these vibrations correspond to the furan and thiophene rings being oriented perpendicular to the surface. The spectral behavior of the TAF system differed, and the corresponding bands observed at 1407 and 1282 cm^{-1} maintained the same intensity due to the surface effect but shift to 1391 and 1294 cm^{-1}, respectively. Therefore, the position of the νCC modes of both thiophene and furan that are rather perpendicular to the surface is closer to the surface. A similar situation is proposed for the SERS bands at 1271, 1183 and 1161 cm^{-1} of TAF, the last two bands coupled to CH in plane deformations. The bands due to in-plane modes in the 1100–900 cm^{-1} range corresponding to the anthracene ring were not enhanced due to the surface effect which indicates that the ring is far from the surface and parallel to the surface. The band at 1217 cm^{-1} in TAT and at 1222 cm^{-1} in FAF due to νCC/δCH of anthracene disappeared by surface effect. The above results support the fact that the most probable orientation of the anthracene moiety is parallel to the surface and the substituents remains perpendicular to the surface. One of the observed spectral changes caused by the surface effect in the 670–700 cm^{-1} region was associated to ring deformations involving the OCO and OCS moieties. The TAT double band with maxima at 672 and 664 cm^{-1} is observed in SERS at 670 cm^{-1} with medium relative intensity, supporting the perpendicular position of the thiophene ring on the surface. The fact that the band at 664 cm^{-1} is not observed in SERS could be associated to CH out of plane deformations of thiophene or furane. Fig. 3 shows the 200–600 cm^{-1} region: The anthracene SERS bands located at approximately 400 and 478 cm^{-1} due to out-of-plane ring deformations maintain their Raman intensities, which supports the hypothesis regarding the planar parallel orientation of the anthracene ring on the gold surface. The Raman bands at 430 cm^{-1} for FAF, 422 cm^{-1} for TAT, and 426 cm^{-1} for TAF, are observed with similar wavenumbers in SERS, suggesting modes vibrating close to the surface. For TAF and FAF, the band near 370 cm^{-1} appearing by surface effect (Fig. 3) may be related to the νAuO mode following that reported for dimethylgold(III) carboxylates where this vibration was observed in the 500–250 cm^{-1} region [39]. Both the νAuO and νAuS vibrations were observed in the SERS spectrum of TAF at 369 and 276 cm^{-1}, respectively. The last SERS band was broad and weak for TAF and very weak for FAF (see Fig. 3); the weak intensity is related to a feeble analyte-surface interaction. According to Razmutė-Razmė et al. [40] and Sanchez et al. [41]. The Raman bands at 241 and 235 cm^{-1} observed only in TAF and FAF maintain the relative intensity and wavenumbers by surface effect which suggests that they belong to furan ring vibrations close to the metal surface. The Raman bands located at 226 cm^{-1} in TAT and 222 cm^{-1} in TAF attributed to a thiophene ring deformation mode, are not observed by surface effect; assuming that the thiophene ring is perpendicular to the surface the molecular ring fragment is far from the surface or the corresponding mode has the α_{zz} component parallel to the surface [13]. On the

basis of a similar argument the SERS band at 202 cm^{-1} should correspond to a thiophene ring mode vibrating close to the surface.

3.3. Theoretical calculations

In the isolated gold layer, the valence and conduction bands overlap, indicating that the microscopic model employed here is a good representation of a metallic cluster. Also, the Au layer has not the HOMO and LUMO (that can be considered respectively as being closer to the upper part of the valence band and the lower part of the conduction band of the cluster) localized on its center.

3.3.1. TAT molecular system

The results in Fig. 4a indicate that each sulfur atom has three Au-S interactions (3.13, 3.21, 3.22, 3.13, 3.22 and 3.21 Å). The rings of the central anthracene system are not coplanar due to the pentagonal substituents. The EHT and DFT results show that the HOMO and LUMO of TAT are localized on the anthracene moiety and have very small localization on the sulfur atoms that are parallel to the gold surface. Therefore, we cannot expect charge transfer from the S atoms to the surface. Due to the distance between the anthracene moiety and the surface, no charge transfer process is expected. In addition, no overlap occurs between the frontier MOs of the partners. Therefore, the electrostatic forces most likely dominate the TAT-surface interaction.

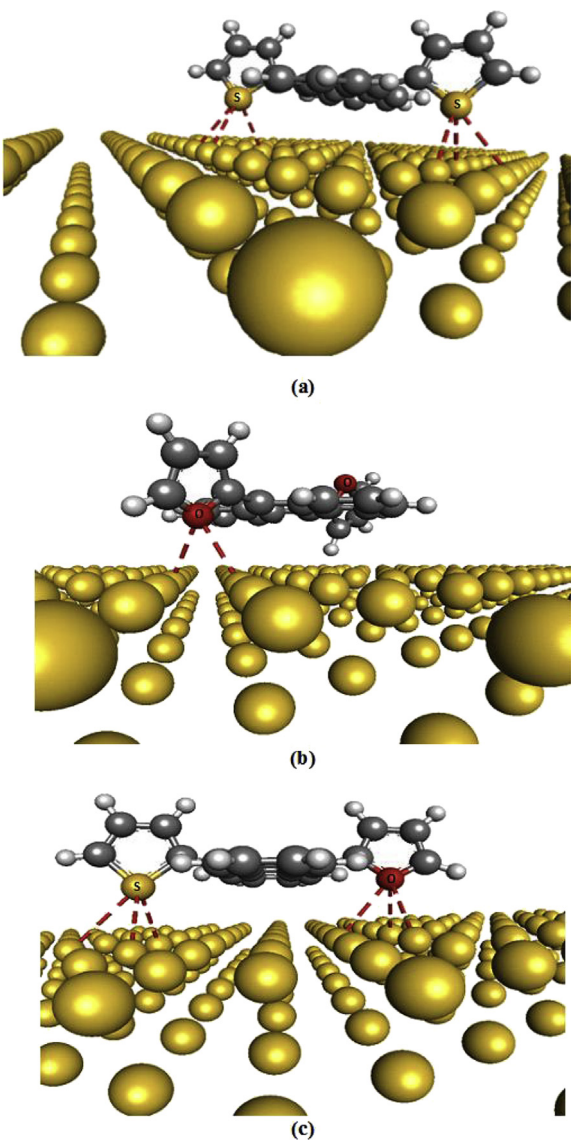

Fig. 4. Predicted molecular model for the (a) TAT (b) FAF (c) TAF-gold surface interaction.

3.3.2. FAF molecular system

As shown in Fig. 4b, for FAF, two interactions were observed between the oxygen atom of furan and the Au surface (2.83 and 2.84 Å). The EHT results, which were confirmed by B3LYP/6-31G(d,p) calculations with full geometry optimization, indicate that the HOMO is not localized on the oxygen atoms and the LUMO has a very small electronic density on these atoms. Moreover, the HOMO and LUMO are localized on the anthracene moiety and very far from the surface due to the two perpendicular pentagonal rings. These orbitals do not overlap with the frontier MOs of the Au layer. Therefore, charge transfer from the molecule to the surface and vice versa may be discarded. However, the electrostatic forces appear to dominate the FAF-metal surface interaction.

3.3.3. TAF molecular system

Fig. 4c shows six molecule-surface interactions. Three of these interactions correspond to Au-S (3.31, 3.19 and 3.18 Å). The remaining interactions are Au-O interactions (2.94, 3.07 and 3.15 Å). Importantly, the gold-sulfur interaction distance was calculated to be close to the 2.6 Å, which is consistent with that thiophenols adsorbed on gold [42]. The furan, thiophene and the central anthracene rings are not coplanar. For FAF, the calculations indicate that the HOMO is not localized on the oxygen and sulfur atoms. In addition, the LUMO has a very small electronic density on these atoms. Similar to previous cases, no overlap was observer between the frontier MOs of the partners. Charge transfer between the molecule and the surface can be ignored. However, electrostatic forces appear to predominate the TAF-surface interaction.

If the TAT and FAF molecules are oriented as shown in Fig. 4a and b and are on a hot spot and the laser line is perpendicular to the surface, the coupled in-plane δCH/νCC mode of anthracene should disappear due to the surface effect according to the SERS selection rules [13], which is the case for the band at about 1220 cm^{-1}. In addition, the equivalent coupled mode for TAF, (Fig. 4c) should be intense in SERS, which is the case for the band at 1219 cm^{-1}. A similar situation is related to the out of plane ring modes of anthracene, (i.e., the bands at approximately 480 and 400 cm^{-1} in the Raman spectrum); the intensity of these Raman bands is predicted to increase due to the surface effect, which was confirmed by the SERS spectrum where these bands were observed with medium weak intensities.

4. Conclusions

The 9,10-di(thiophen-2-yl)anthracene (TAT), 9,10-di(furan-2-yl) anthracene (FAF) and 2-[(10-(thiophen-2-yl)anthracen-9-yl)]furan (TAF) cruciform molecular systems were synthesized and structurally characterized. The Raman and surface-enhanced Raman scattering (SERS) data allowed us to propose that the ligands interact with the gold surface primarily through the heterocycles, especially through the O and S atoms. The rings of the anthracene fragment are not exactly coplanar, and the anthracene ring moiety is far from the surface and maintains a parallel orientation on the surface. The substituents are out of the anthracene plane and tilted with respect to the gold surface. The calculations provide a good representation of the experimental data. Based on these results, the ligand-metal surface interaction is proposed to be dominated by electrostatic forces rather than formal bonding. The calculated distances are 3.3–3.1 Å for Au-S and 2.8–3.1 Å for Au-O.

Acknowledgements

P. Leyton and M. Campos-Vallette acknowledge the FONDECYT 1140810 and 1140524 projects as well as the as FONDEQUIP EQM130170 project from CONICYT. This article is devoted to J. Brunet who is retiring after a long and productive scientific career, we appreciate all his advices and life teachings.

Appendix A. Supplementary data

Supplementary data related to this article can be found at http://dx.doi.org/10.1016/j.molstruc.2016.06.002.

References

[1] Q. Shen, X. Guo, M.L. Steigerwald, C. Nuckolls, Integrating reaction chemistry into molecular electronic devices, Chem. Asian J. 5 (2010) 1040–1057, http://dx.doi.org/10.1002/asia.200900565.
[2] S. Park, M.J. Weaver, A versatile surface modification scheme for attaching metal nanoparticles onto gold: characterization by electrochemical infrared spectroscopy, J. Phys. Chem. B 106 (2002) 8667–8670, http://dx.doi.org/10.1021/Jp025957y.
[3] A.N. Shipway, E. Katz, I. Willner, Nanoparticle arrays on surfaces for electronic, optical, and sensor applications, Chem. Phys. Chem. 1 (2000) 18–52, http://dx.doi.org/10.1002/1439-7641(20000804)1, 1<18::AID-CPHC18>3.0.CO;2-L.
[4] J.E. Klare, G.S. Tulevski, K. Sugo, A. De Picciotto, K.A. White, C. Nuckolls, Cruciform pi-systems for molecular electronics applications, J. Am. Chem. Soc. 125 (2003) 6030–6031, http://dx.doi.org/10.1021/ja0350942.
[5] J.E. Klare, G.S. Tulevski, C. Nuckolls, Chemical reactions with upright monolayers of cruciform π-systems, Langmuir 20 (2004) 10068–10072, http://dx.doi.org/10.1021/la0479152.
[6] H. Kang, P. Zhu, Y. Yang, A. Facchetti, T.J. Marks, Self-assembled electrooptic thin films with remarkably blue-shifted optical absorption based on an X-shaped chromophore, J. Am. Chem. Soc. 126 (2004) 15974–15975, http://dx.doi.org/10.1021/ja045043k.
[7] J.K. Sorensen, M. Vestergaard, A. Kadziola, K. Kilså, M.B. Nielsen, Synthesis of oligo(phenyleneethynylene)-tetrathiafulvalene cruciforms for molecular electronics, Org. Lett. 8 (2006) 1173–1176, http://dx.doi.org/10.1021/ol060071o.
[8] Q. Jin, J.A. Rodriguez, C.Z. Li, Y. Darici, N.J. Tao, Self-assembly of aromatic thiols on Au(111), Surf. Sci. 425 (1999) 101–111, http://dx.doi.org/10.1016/S0039-6028(99)00195-8.
[9] C. Vericat, M.E. Vela, G. Benitez, P. Carro, R.C. Salvarezza, Self-assembled monolayers of thiols and dithiols on gold: new challenges for a well-known system, Chem. Soc. Rev. 39 (2010) 1805–1834, http://dx.doi.org/10.1039/b907301a.
[10] M. Buck, M. Grunze, M. Zharnikov, A. Shaporenko, Y. Tai, H.-T. Rong, W. Eck, Fabrication of thiol-terminated surfaces using aromatic self-assembled monolayers, J. Phys. Chem. B 108 (2004) 16806–16810, http://dx.doi.org/10.1021/jp0402380.
[11] S.W. Joo, S.W. Han, K. Kim, Adsorption characteristics of p -Xylene-α,α'-dithiol on gold and silver surfaces: surface-enhanced Raman scattering and ellipsometry study, J. Phys. Chem. B 103 (1999) 10831–10837, http://dx.doi.org/10.1021/jp992230+.
[12] F.K. Huang, R.C. Horton Jr., D.C. Myles, R.L. Garrell, Selenolates as alternatives to thiolates for self-assembled monolayers: a SERS study, Langmuir 14 (1998) 4802–4808, http://dx.doi.org/10.1021/la980263v.
[13] M. Moskovits, Surface-enhanced spectroscopy, Rev. Mod. Phys. 57 (1985) 783–825.
[14] M. Moskovits, D.P. DiLella, K.J. Maynard, Surface Raman spectroscopy of a number of cyclic aromatic molecules adsorbed on silver: selection rules and molecular reorientation, Langmuir 4 (1988) 67–76, http://dx.doi.org/10.1021/la00079a012.
[15] P. Leyton, C. Domingo, S. Sánchez-Cortés, M. Campos-Vallette, J.V. Garcia-Ramos, Surface enhanced vibrational (IR and Raman) spectroscopy in the design of chemosensors based on ester functionalized p-tert-butylcalix[4]arene hosts, Langmuir 21 (2005) 11814–11820, http://dx.doi.org/10.1021/la051761o.
[16] P. Leyton, J.S. Gómez-Jeria, S. Sánchez-Cortés, C. Domingo, M. Campos-Vallette, Carbon nanotube bundles as molecular assemblies for the detection of polycyclic aromatic hydrocarbons: surface-enhanced resonance Raman spectroscopy and theoretical studies, J. Phys. Chem. B 110 (2006) 6470–6474, http://dx.doi.org/10.1021/jp056379z.
[17] U.K. Sarkar, A pH-dependent SERS study of thiophene-2-carboxylic acid adsorbed on Ag-sols, Chem. Phys. Lett. 374 (2003) 341–347, http://dx.doi.org/10.1016/S0009-2614(03)00728-0.
[18] T. Iliescu, F.D. Irimie, M. Bolboaca, C. Paisz, W. Kiefer, Surface enhanced Raman spectroscopy of 5-(4-fluorophenyl)-furan-2 carbaldehyde adsorbed on silver colloid, Vib. Spectrosc. 29 (2002) 251–255.
[19] J. Bukowska, K. Jackowska, SERS spectra as evidence of pyrrole and thiophene polymerization on silver electrodes, Synth. Met. 35 (1990) 135–142, http://dx.doi.org/10.1016/0379-6779(90)90036-K.
[20] J. Kimling, M. Maier, B. Okenve, V. Kotaidis, H. Ballot, A. Plech, Turkevich method for gold nanoparticle synthesis revisited, J. Phys. Chem. B 110 (2006) 15700–15707, http://dx.doi.org/10.1021/jp061667w.
[21] M. Durso, M. Zambianchi, A. Zanelli, M.G. LoBello, F. De Angelis, S. Toffanin, S. Cavallini, D. Gentili, F. Tinti, M. Cavallini, N. Camaioni, M. Melucci, Synthesis by MW-assisted direct arylation, side-arms driven self-assembly and functional properties of 9,10-dithienylanthracene orthogonal materials, Tetrahedron 70 (2014) 6222–6228, http://dx.doi.org/10.1016/j.tet.2014.03.010.
[22] S. Kotha, A.K. Ghosh, K.D. Deodhar, Synthesis of symmetrical and unsymmetrical 9,10-diarylanthracene derivatives via Bis-Suzuki-Miyaura cross-coupling reaction, Synth. (Stuttg.) (2004) 549–557, http://dx.doi.org/10.1055/s-2004-815981.
[23] Hypercube Inc., HyperChem(TM) Professional, 2002, 1115 NW 4th Street Gainesville, Florida 32601, USA.
[24] M.J. Frisch, G.W. Trucks, H.B. Schlegel, G.E. Scuseria, M.A. Robb, J.R. Cheeseman, G. Scalmani, V. Barone, B. Mennucci, G.A. Petersson, H. Nakatsuji, M. Caricato, X. Li, H.P. Hratchian, A.F. Izmaylov, J. Bloino, G. Zheng, J.L. Sonnenberg, M. Hada, M. Ehara, K. Toyota, R. Fukuda, J. Hasegawa, M. Ishida, T. Nakajima, Y. Honda, O. Kitao, H. Nakai, T. Vreven, J.A.J. Montgomery, J.E. Peralta, F. Ogliaro, M. Bearpark, J.J. Heyd, E. Brothers, K.N. Kudin, V.N. Staroverov, R. Kobayashi, J. Normand, K. Raghavachari, A. Rendell, J.C. Burant, S.S. Iyengar, J. Tomasi, M. Cossi, N. Rega, J.M. Millam, M. Klene, J.E. Knox, J.B. Cross, V. Bakken, C. Adamo, J. Jaramillo, R. Gomperts, R.E. Stratmann, O. Yazyev, A.J. Austin, R. Cammi, C. Pomelli, J.W. Ochterski, R.L. Martin, K. Morokuma, V.G. Zakrzewski, G.A. Voth, P. Salvador, J.J. Dannenberg, S. Dapprich, A.D. Daniels, Ö. Farkas, J.B. Foresman, J.V. Ortiz, J. Cioslowski, D.J. Fox, Gaussian 09, Revision A.1, 2010.
[25] A.M. Vera, J.J. Cárcamo, A.E. Aliaga, J.S. Gómez-Jeria, M.J. Kogan, M.M. Campos-Vallette, Interaction of the CLPFFD peptide with gold nanospheres. A Raman, surface enhanced Raman scattering and theoretical study, Spectrochim. Acta A. Mol. Biomol. Spectrosc. 134 (2015) 251–256, http://dx.doi.org/10.1016/j.saa.2014.06.116.
[26] M.A. Herrera, G.P. Jara, R. Villarroel, A.E. Aliaga, J.S. Gómez-Jeria, E. Clavijo, C. Garrido, T. Aguayo, M.M. Campos-Vallette, Surface enhanced Raman scattering study of the antioxidant alkaloid boldine using prismatic silver nanoparticles, Spectrochim. Acta A. Mol. Biomol. Spectrosc. 133 (2014) 591–596, http://dx.doi.org/10.1016/j.saa.2014.05.070.
[27] A.E. Aliaga, C. Garrido, P. Leyton, G. Diaz, J.S. Gómez-Jeria, T. Aguayo, E. Clavijo, M.M. Campos-Vallette, S. Sánchez-Cortés, SERS and theoretical studies of arginine, Spectrochim. Acta - Part A Mol. Biomol. Spectrosc. 76 (2010) 458–463, http://dx.doi.org/10.1016/j.saa.2010.01.007.
[28] A.E. Aliaga, H. Ahumada, K. Sepúlveda, J.S. Gómez-Jeria, C. Garrido, B.E. Weiss-López, M.M. Campos-Vallette, SERS, molecular dynamics and molecular orbital studies of the MRKDV peptide on silver and membrane surfaces, J. Phys. Chem. C 115 (2011) 3982–3989, http://dx.doi.org/10.1021/jp1107153.
[29] P. Leyton, I. Córdova, P.A. Lizama-Vergara, J.S. Gómez-Jeria, A.E. Aliaga, M.M. Campos-Vallette, E. Clavijo, J.V. García-Ramos, S. Sánchez-Cortés, Humic acids as molecular assemblers in the surface-enhanced Raman scattering detection of polycyclic aromatic hydrocarbons, Vib. Spectrosc. 46 (2008) 77–81, http://dx.doi.org/10.1016/j.vibspec.2007.10.006.
[30] T. Aguayo, C. Garrido, R.E. Clavijo, J.S. Gómez-Jeria, C. Araya Monasterio, M. Icaza, F. Espinoza Moraga, M.M. Campos Vallette, Raman and surface enhanced Raman scattering of a black dyed silk, J. Raman Spectrosc. 44 (2013) 1238–1245, http://dx.doi.org/10.1002/jrs.4348.
[31] A.E. Aliaga, T. Aguayo, C. Garrido, E. Clavijo, E. Hevia, J.S. Gómez-Jeria, P. Leyton, M.M. Campos-Vallette, S. Sánchez-Cortés, Surface-enhanced Raman scattering and theoretical studies of the C-terminal peptide of the β-subunit human chorionic gonadotropin without linked carbohydrates, Biopolymers 95 (2011) 135–143, http://dx.doi.org/10.1002/bip.21542.
[32] D. Lin-Vien, N.B. Colthup, W.G. Fateley, J.G. Grasselli, The Handbook of Infrared and Raman Characteristic Frequencies of Organic Molecules, Academic Press, Boston, 1991.
[33] G. Socrates, Infrared and Raman Characteristic Group Frequencies, Tables and Charts, third ed., John Wiley & Sons, Chichester, 2001.
[34] J. Kwiatkowski, J. Leszczynski, I. Teca, Molecular structure and infrared spectra of furan, thiophene, selenophene and their 2,5-N and 3,4-N derivatives: density functional theory and conventional post-Hartree-Fock MP2 studies, J. Mol. Struct. 436–437 (1997) 451–480, http://dx.doi.org/10.1016/S0022-2860(97)00125-7.
[35] R. Kalescky, E. Kraka, D. Cremer, Description of aromaticity with the help of vibrational spectroscopy: anthracene and phenanthrene, J. Phys. Chem. A 118 (2014) 223–237, http://dx.doi.org/10.1021/jp4092514.
[36] B.V. Lokshin, N.E. Borisova, B.M. Senyavin, M.D. Reshetova, Analysis of vibrational spectra of naphthalene, deuterionaphthalenes, and chromium (η6-naphthalene)tricarbonyl based on density functional calculations, Russ. Chem. Bull. 51 (2002) 1656–1666. http://www.scopus.com/scopus/inward/record.url?eid=2-s2.0-0036448985&partnerID=40&rel=R8.0.0.
[37] A. Srivastava, V.B. Singh, Theoretical and experimental studies of vibrational spectra of naphthalene and its cation, Indian J. Pure Appl. Phys. 45 (2007) 714–720.
[38] A.A. El-Azhary, R.H. Hilal, Vibrational analysis of the spectra of furan and thiophene, Spectrochim. Acta, Part A 53 (1997) 1365–1373, http://dx.doi.org/10.1016/S1386-1425(97)00051-6.

[39] A.A. Bessonov, T.V. Basova, V.G. Kiselev, L.A. Sheludyakova, N.B. Morozova, I.K. Igumenov, Vibrational interactions in dimethylgold(III) halides and carboxylates, Vib. Spectrosc. 51 (2009) 283–288, http://dx.doi.org/10.1016/j.vibspec.2009.07.003.

[40] I. Razmute-Razme, Z. Kuodis, O. Eicher-Lorka, G. Niaura, In-situ surface-enhanced Raman spectroscopic investigation of NH site of indole ring-terminated self-assembled monolayer on gold electrode, Chemija 18 (2007) 16–20.

[41] J. Kubackova, I. Izquierdo-Lorenzo, D. Jancura, P. Miskovsky, S. Sánchez-Cortés, Adsorption of linear aliphatic α,ω-dithiols on plasmonic metal nanoparticles: a structural study based on surface-enhanced Raman spectra, Phys. Chem. Chem. Phys. 16 (2014) 11461–11470, http://dx.doi.org/10.1039/c4cp00424h.

[42] S. Miranda-Rojas, A. Muñoz-Castro, R. Arratia-Pérez, F. Mendizábal, Theoretical insights into the adsorption of neutral, radical and anionic thiophenols on gold(111), Phys. Chem. Chem. Phys. 15 (2013) 20363–20370, http://dx.doi.org/10.1039/c3cp53591f.